Title: Collision induced dissociation study of the major components of silymarin

Authors: Ákos Kuki, Bernadett Biri, Lajos Nagy, György Deák, József Kalmár, Attila Mándi, Miklós Nagy, Miklós Zsuga, Sándor Kéki

PII: S1387-3806(12)00101-7
DOI: doi:10.1016/j.ijms.2012.02.021
Reference: MASPEC 14674

To appear in: *International Journal of Mass Spectrometry*

Received date: 12-1-2012
Revised date: 22-2-2012
Accepted date: 24-2-2012

Please cite this article as: Á. Kuki, B. Biri, L. Nagy, G. Deák, J. Kalmár, A. Mándi, M. Nagy, M. Zsuga, S. Kéki, Collision induced dissociation study of the major components of silymarin, *International Journal of Mass Spectrometry* (2010), doi:10.1016/j.ijms.2012.02.021

*Graphical Abstract

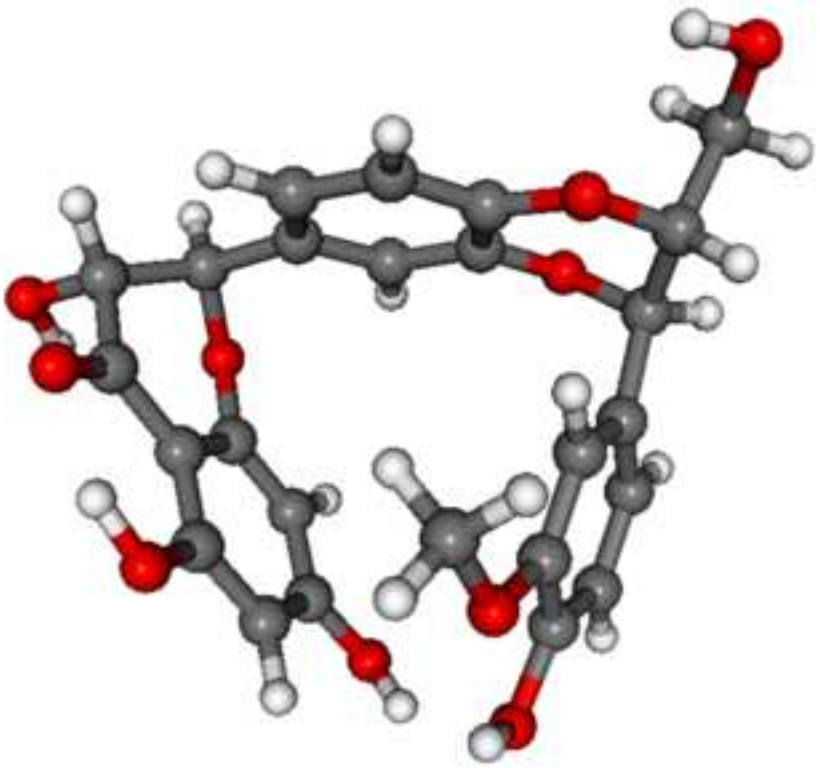

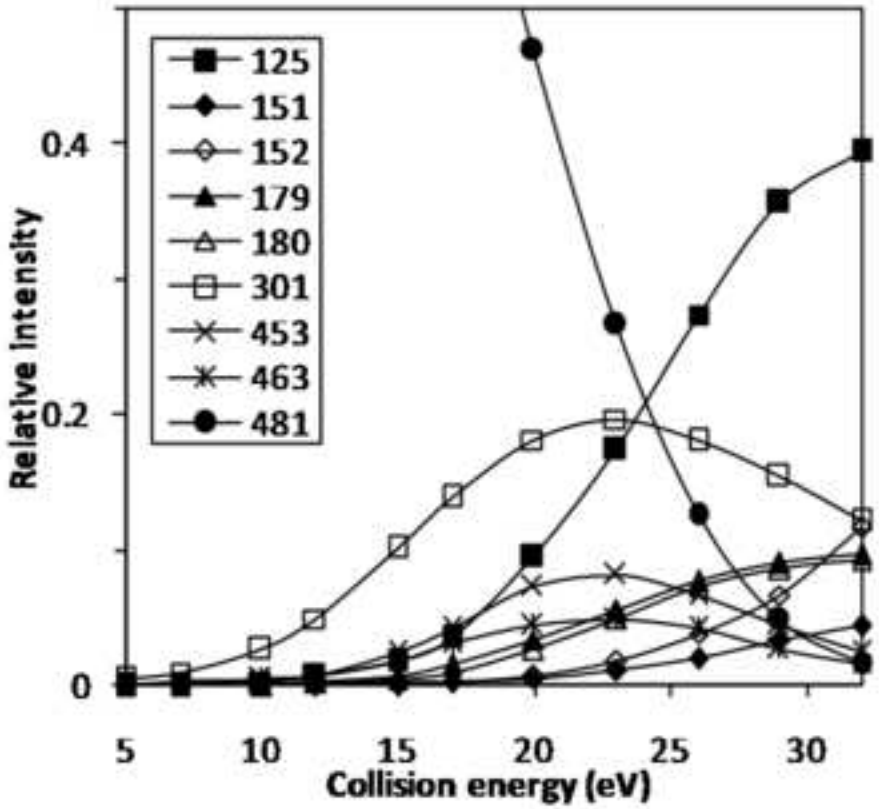

Collision induced dissociation study of the major components of silymarin

Ákos Kuki[1], Bernadett Biri[1], Lajos Nagy[1], György Deák[1], József Kalmár[2], Attila Mándi[3], Miklós Nagy[1], Miklós Zsuga[1], Sándor Kéki[1]*

[1]*Department of Applied Chemistry, University of Debrecen, Hungary,*
[2]*Department of Inorganic and Analytical Chemistry, University of Debrecen, Hungary*
[3]*Department of Organic Chemistry, University of Debrecen, Hungary*

* Corresponding author: keki.sandor@science.unideb.hu, tel: +36 52 518662/22455; fax: +36 52 518662; *H-4010 Debrecen, Hungary*

Abstract

The fragmentation properties of the major silymarin constituents, including silydianin, silychristin A and B, silybin A and B and isosilybin A and B were studied by energy-dependent collision-induced dissociation (CID) technique. The survival yield (SY) method was applied to compare the fragmentation behavior of the various silymarin components. MS/MS spectra were recorded at collision energies which correspond to about 50% survival yield (CE_{50}) and about 1% survival yield (CE_{01}). The laboratory frame collision energy dependence of the fragmentation was studied on the basis of the breakdown curves, i.e., the relative intensities of fragment ions *versus* collision energy. The fragmentation of silybins and isosilybins are distinct in spite of the minimal difference between their structures. This phenomenon, which is the basis of their analytical identification, is explained in details for the first time, on the basis of the energy-dependent MS/MS experiments and the conformational analysis.

Keywords: milk thistle, silymarin, silybin, energy dependent collision-induced dissociation, survival yield, breakdown curve

Introduction

Silymarin is a mixture of flavanolignans extracted from milk thistle (*Silybum marianum*) seeds with pharmacological relevance.[1-4] Natural silymarin is used in the therapy of liver diseases because of its hepatoprotective effect. The silybins, the major components of silymarin, display highly efficient anti-tumor, anti-inflammatory and anti-fibrotic activity.[5-9] The qualitative and quantitative analysis of the natural extract is based on liquid chromatography-mass spectrometry (LC-MS) methods with soft ionization e.g., electrospray (ESI).[10] In our recent study eleven active components of silymarin with the same elemental composition were separated by traditional reverse phase liquid chromatography.[11] Furthermore, we defined simple criteria for distinguishing between the major components by simple MS/MS experiments. Rapid separation and fragmentation of the main bioactive constituents in silymarin has also been reported by Wang et al. by UPLC-ESI-MS.[12] The fragmentation behavior of the major components including silychristin A and B, silydianin, silybin A and B, isosilybin A and B (see the structures in Scheme 1) has been studied under different conditions.[13,14] Shibano et al. studied the collision-induced dissociation using MS/MS and MS^3 techniques by hybrid ion-trap and time-of-flight (IT-TOF) mass spectrometry.[15] A detailed dissociation study of silybin and its main structural blocks has been published. This work utilized atmospheric pressure chemical ionization quadrupole time-of-flight tandem mass spectrometry (APCI-Q-TOF) in positive ion mode.[16]

In spite of the considerable number of previous reports, the energy dependence of the fragmentation of the silymarin constituents was not studied. In this work we report a detailed energy dependent collision induced dissociation (CID) MS/MS fragmentation study of the mentioned seven major compounds (including only the *trans* isomers where applies, *vide infra*). The ambiguous fragment ion structures reported previously are reinvestigated and clarified. We also propose an explanation for the distinct fragmentation behavior of silybins and isosilybins, two major groups of compounds the structures of which differ only in the relative position of 2 substituents.

Scheme 1

Material and methods

Chemicals

HPLC grade hexane (Molar Chemicals, Budapest, Hungary), acetonitrile (Merck, Darmstadt, Germany), dichloromethane (Scharlau, Sentmenat, Spain), methanol (WWR International,

Leuven, Belgium) and formic acid (Scharlau, Sentmenat, Spain) were used without further purification. Water was purified by a Direct-Q water system (Millipore, Molsheim, France).

Sample preparation and HPLC separation

The preparation of the silymarin samples was achieved according to reference [17].

The ripe *Silybum marianum* seeds were collected in the region of Arad, Romania in 2010. 1200 g dried seed was powdered, homogenized and defatted by hexane in a Soxhlet extractor for 6 h. The defatted powder was dried and then macerated with acetonitrile at room temperature for 6 h. The solvent was evaporated and the crude silymarin was washed with ice-cold dichloromethane. To prepare stock solution for the HPLC analysis the dried silymarin was dissolved in methanol at a concentration of 1 mg/mL and was injected onto the LC–MS/MS for analysis. The yield of silymarin was 40 g, which is 3.3 % w/w of the initial ripe seed.

For chromatography a Waters 2695 Separation Module was used, equipped with a termostable autosampler (5°C) module, a column module (40°C), a Waters 2996 Photodiode-array detector and a Waters Symmetry C18 column (4.6×150 mm, 3.5 μm) (each from Waters, Milford, USA). The analytes were detected at 225 and 288 nm. The gradient chromatographic method was reported in our previous paper.[11]

Electrospray Quadrupole Time-of-Flight MS/MS (ESI-Q-TOF).

The MS/MS measurements were performed with a MicroTOF-Q type Qq-TOF MS instrument (Bruker Daltonik, Bremen, Germany) using an ESI source with negative ion mode. The spray voltage was set to 4 kV. The temperature of the drying gas (N_2) was kept at 180 °C. For the MS/MS experiments, nitrogen was used as the collision gas and the collision energies were varied in the range from 5 eV to 32 eV (in the laboratory frame). The pressure in the collision cell was determined to be 8×10^{-3} mbar. The precursor ions for MS/MS were selected with an isolation width of *m/z* 4. The MS/MS spectra were accumulated and recorded by means of a digitizer at a sampling rate of 2 GHz. The mass spectra were calibrated externally using the exact masses of the clusters generated from the electrosprayed solution of sodium trifluoroacetate (NaTFA). The recorded mass spectra were evaluated with the DataAnalysis 3.4 software from Bruker.

Evaluation of the survival yield curves

The efficiency of the fragmentation can be quantitatively described by the survival yield (SY).[18-20] The SY is defined according to eq 1:

$$SY = \frac{I_p}{I_p + \sum I_f} \quad (1)$$

where I_p is the intensity of the precursor ion, and ΣI_f is the sum of all the fragment ion intensities. The shape of the SY *versus* laboratory frame collision energy (CE) curve is sigmoidal. The collision energy at which the intensity of the precursor ion is equal to the sum of that of all the fragment ions (i.e., SY = 0.5) was determined with appropriate accuracy by a linear two-point interpolation.[21] The standard deviation is 0.1 eV and the relative error in percentage is 0.5 %. This energy is noted as characteristic collision energy (CE_{50}).

Computational Section

Mixed torsional/low mode conformational searches were carried out for silybin A (**4**) and isosilybin A (**6**) by means of the Macromodel 9.7.211 [22] software using Merck Molecular Force Field (MMFF) in vacuo. The MMFF analysis provided more than 2000 conformers for both compounds in an 84 kJ/mol energy window, from which the first 21 kJ/mol range, all „double diaxial" conformers and the lowest energy conformers of the further clusters were then reoptimized at the B3LYP/6-31G (d) level of theory implemented in the Gaussian 09 [23] package. The MOLEKEL [24] software package was used for visualization of the results.

Results and Discussion

In our previous study, an HPLC-ESI MS/MS method was developed for the separation and characterization of the constituents of silymarin. The UV chromatogram and the extracted ion chromatogram at *m/z* 481 ($[M–H]^-$) of silymarin are already reported.[11] The 2,3-*cis* stereoisomers of the components have completely identical fragmentation properties,[11] thus only the *trans* isomers will be described henceforth. The following seven major active components of silymarin with the same elemental composition were completely separated and analyzed by energy dependent CID MS/MS technique: silychristin A (**1**), silychristin B (**3**), silydianin (**2**), silybin A (**4**), silybin B (**5**), isosilybin A (**6**), isosilybin B (**7**) (Scheme 1). The SY method was used for the evaluation of the energy dependence of the fragmentation processes, the CE_{50} values were determined as detailed in the experimental section. The SY

versus CE diagrams of all the studied silymarin components are presented in Fig 1, and the associated CE_{50} values are compiled in Table 1.

Fig 1

Table 1

As seen in Fig 1, the SY plots of silydianin (**2**), the silybins (**4**, **5**) and the isosilybins (**6**, **7**) coincide with each other, while the SY plots of the silychristins (**1**, **3**) are shifted to lower energies, with about 5 eV characteristic collision energy.

Comparison of the appearance and relative abundances of the fragment ions from the precursor *m/z* 481 ($[M–H]^-$) serves as an effective tool for the identification of the different flavonolignans in silymarin. Previous studies compiled LC-MS/MS CID spectra of all the silymarin constituents detected at one given value of collision energy. For the characterization of the silymarin components herein we utilized the MS/MS spectra corresponding to 50% fragmentation, namely recorded at CE_{50}, where the degree of fragmentation reactivity is similar. We propose that in a series of experiments the collision energies should be chosen to result the same SY (e.g., to be CE_{50}) regardless of the analyte, because with this method both the product ion spectra of the different compounds and the spectra of the same compound recorded by different instruments become more comparable. The ESI MS/MS spectra of silychristin A (**1**), silydianin (**2**), silybin A (**4**) and isosilybin A (**6**) recorded at CE_{50} are displayed in Fig 2a. It was shown in our previous report, that the MS/MS spectra of the 2 silychristin diastereomers (**1**, **3**), the 2 silybin diastereomers (**4**, **5**) and the 2 isosilybin diastereomers (**6**, **7**) are identical as listed in respective pairs.[11] Thus only four product ion spectra are shown for the seven components.

Fig 2

As seen in Fig 2a, the most intensive product ions at CE_{50} are different for each silymarin constituents. The most abundant product ions are: *m/z* 451 for the silychristins (**1**, **3**), *m/z* 151 for silydianin (**2**), *m/z* 301 for the silybins (**4**, **5**) and *m/z* 453 for the isosilybins (**6**, **7**). The dissimilarity can be utilized for the rapid identification of the silymarin constituents, provided that the CE_{50} values are determined.[11]

At the CE_{50} values, which are in the range from 14 eV to 20 eV, the low-energy fragments are more abundant than the fragments originating from the consecutive reactions. By increasing

the collision energy, the consecutive reactions become more dominant and the product ion spectra significantly change. The ESI MS/MS spectra of silychristin A (**1**), silydianin (**2**), silybin A (**4**), isosilybin A (**6**) recorded at the collision energies corresponding to SY ≈ 0.01, noted CE_{01}, are shown in Fig 2b. Albeit the spectrum at CE_{01} contains more structural information, the spectrum recorded at CE_{50} is more useful for the rapid identification of the silymarin constituent. Theoretical masses, elemental compositions and proposed structures for the major fragment ions are shown in Table 2.

Table 2

In order to gain deeper insight into the fragmentation behavior of the silymarin constituents the breakdown curves, i.e., the relative intensities of fragment ions *versus* collision energy plots were constructed. For example in the collision energy range of 5-32 eV, the most abundant ions are at *m/z* 151 and 179 for silydianin (**2**), while those for silybin A (**4**) are at *m/z* 125 and 301. This difference is reasonable considering the dissimilarity of their structures. Interestingly the intensities of the fragment ions of the silybins (**4**, **5**) and the isosilybins (**6**, **7**) are also different, in spite of their closely similar structures. The difference is not only the distinguishing ratio of the fragment ions *m/z* 301 and *m/z* 453, but new fragment ions appear in the spectra of the silybins, e.g., at *m/z* 451. The substituents of C(10) and C(11) in the silybin A (**4**) and isosilybin A (**6**) are exchanged, however in the most stable conformations they are far from C(4), which carbon atom is leaving as CO resulting the fragment ion *m/z* 453. Based on energy-dependent dissociation studies we report the detailed mechanisms of these diverse fragmentations.

Fig 3

The comparison of the breakdown curves of fragment ions *m/z* 301, 451 and 453 from the silybin and isosilybin precursors is seen in Fig 3. We assume that the distinct fragmentation behavior is due to the increased stability of a semi-stable conformation of silybins compared to isosilybins. MMFF conformational analysis of silybin A (**4**) and isosilybin A (**6**) were carried out, which provided 2493 and 2349 conformers respectively in an 84 kJ/mol energy window. The resulting conformers were clustered into 4 groups according to the conformation of the C and D ring moieties. In the most stable form rings C and D have diequatorial twist boat conformation. Two other groups mean, that only one of the rings has diequatorial

conformation, while the other has diaxial. The last group, where both C and D rings were found to be in diaxial twist boat form has 18-18 conformers in the case of silybin A (**4**) and isosilybin A (**6**). These conformations were then also reoptimized at the B3LYP/6-31G (d) level of theory. The relative B3LYP energies of the most stable conformers from the 4 groups are compared in Table 3 and the atomic coordinates of the 3 dimensional structures can be found in the Supplementary Information.

Table 3

The conformer of silybin A (**4**), where both ring C and D are in diaxial conformation has 27 kJ/mol lower relative energy compared to the analogous conformer of isosilybin A (**6**). Fig 4 shows these possible conformations of silybin A (**4**) compared to the analogous conformations of isosilybin A (**6**).

Fig 4

Silybin A (**4**) can bend into the double diaxial twist boat conformation, ring E can come closer to the chromanon moiety and additional intramolecular H-bonds can form (e.g. between C(7)–OH and C(20)–OH) which stabilize this conformation.

Because of the different constitution of the isosilybins the analogous conformations are not that easily stabilized with intramolecular H-bonds, the double diaxial conformer has significantly higher relative energy, thus the isosilybin is unlikely to be in this conformation.

In the most stable conformers of silybins (**4**, **5**) and isosilybins (**6**, **7**) the hydroxymethyl group on C(10) can form a H-bond with O(9), but in the double diaxial conformers of silybins (**4**, **5**) (e.g. silybin A in Fig 4) this group points outwards, thus the loss of hydroxymethyl group appears at low (10 eV) collision energy. The leaving compound is formaldehyde (*m/z* 30.010), similarly to the fragmentation of the silychristins (**1**, **3**), and the resulting fragment ion is *m/z* 451.105. The initial regions (< 10 eV) of the breakdown curves of *m/z* 301 from the silybins (**4**, **5**) and from the isosilybins (**6**, **7**) are similar, however from 10 eV (i.e., where *m/z* 451.105 appears) the silybins produce relatively more *m/z* 301 than the isosilybins (Fig 3). Based on this observation, the mechanism of the formation of the di-keto fragment ion *m/z* 301 is assumed to be the same in the case of the silybins (**4**, **5**) and isosilybins (**6**, **7**) i.e., the cleavage of two C–O bonds in a retro-Diels-Alder reaction (Scheme 2).

Scheme 2

However, the appearance of the formaldehyde loss from C(10) at 10 eV opens a new reaction pathway for the formation of *m/z* 301 (Scheme 2). Therefore the production of *m/z* 301 becomes faster while the rate of its decay does not change, thus the breakdown curve of this ion in silybins shows higher intensity (Fig 3), namely *m/z* 301 accumulates in the spectra of the silybins (**4**, **5**). In comparison with the literature, previously only simplified assumptions existed, e.g., that the formation of *m/z* 301 fragment ion is unpreferred from isosilybins (**6**, **7**) because of sterical hindrance of the 4-hydroxy-3-methoxyphenyl moiety.[10] Based on our results, the difference in the intensity of the *m/z* 453 peak in the spectra of the silybins (**4**, **5**) and isosilybins (**6**, **7**) can also be explained by the above mentioned stability shift between the double diaxial conformations of the analytes. As seen in Fig 4 the C(4)=O can be sterically hindered and possibly forms an additional intramolecular H-bond in the silybins.

The breakdown diagrams (Fig 5) and the normalized breakdown curves (Supplementary Figure) reveal the differences in the appearance-energies of the various product ions. The fragment ions of silybins (**4**, **5**) and isosilybins (**6**, **7**) can be divided into two groups by the energy of maximum abundance. The ions resulting from the initial fragmentation steps have maximum intensities at around 23 eV, and the fragment ions formed in consecutive reactions have maximum intensities at around 32 eV (Fig 5c). For silychristin A (**1**) the appearance-energies and the energies of maximum intensity for the common fragment ions deviate from this trend (Fig 5a).

Fig 5

The fragment ions *m/z* 463 and 453, which correspond to the loss of H_2O and CO, respectively, are likely formed in a process with relatively low activation energy. Other low-energy fragments are, e.g., the ions *m/z* 451, 433, 355 from the silychristins (Fig 5a), and *m/z* 301 from the silybins and the isosilybins (Fig 5c and d). At higher energies (from 20 eV to 30 eV) the intensities of these ions start to decrease as new pathways of decay open. The product ions which are produced in the processes with the highest activation energies are: *m/z* 151 for the silychristins (**1**, **3**), *m/z* 125 for silydianin (**2**) and *m/z* 152 for the silybins (**4**, **5**) and the isosilybins (**6**, **7**) (Fig5). A precursor dependent energy shift can be observed between the breakdown curves of the fragment ions *m/z* 125 and 179, derived from the chromanone moiety of the flavonolignans. We determined with high mass accuracy, that the accurate mass

of all the *m/z* 179 ions are 178.997 in the spectra of all the silymarin constituents. Thus the elemental composition of *m/z* 179 is unambiguously $C_8H_3O_5$ with the proposed structure shown in Table 2. Previously Lee et. al published that the fragment ion *m/z* 179 from silydianin is $C_8H_3O_5$ in alignment with our results, however a different structure and composition ($C_{10}H_{11}O_3$) with the same nominal mass was proposed for the fragment formed from the silychristins, silybins and isosilybins.[10] As the breakdown diagrams show in Fig 5, the curve of the ion *m/z* 125 is shifted to higher energies compared to that of *m/z* 179 with about 5 eV for the silychristins (**1**, **3**), 3 eV for silydianin (**2**), 2 eV for the silybins (**4**, **5**) and 3 eV for the isosilybins (**6**, **7**).

Conclusions

The collision energy dependence of the fragmentation behavior of the major silymarin constituents was studied by electrospray ionization quadrupole time-of-flight tandem mass spectrometry. The survival yield (SY) plots of silydianin (**2**), the silybins (**4**, **5**) and the isosilybins (**6**, **7**) coincide with each other, while the SY plots of the silychristins (**1**, **3**) are shifted to lower energies with about 5 eV. As the breakdown diagram analysis revealed it is advisable to record the MS/MS spectra of the components at adjusted laboratory frame collision energies to get the same SY value (e.g., 50%) in each case, as this technique ensures higher reproducibility, thus can be utilized for the rapid identification of the silymarin constituents. We also highlighted and explained that a simple substituent exchange can dramatically alter the fragmentation properties as in the case of silybin A (**4**) and isosilybin A (**6**), where the distict fragmentation behavior is due to a stability shift between the possible conformations. The results of the conformational analysis show that the double diaxial conformer of silybin A (**4**) has significantly lower relative energy compared to the analogous conformer of isosilybin A (**6**).

Acknowledgement

This work was financially supported by the grant HURO/0901/058/2.2.2. A. M. thanks the National Information Infrastructure Development Institute (NIIFI 10038), and Dr. T. Kurtán and Dr. I. Komáromi for the helpful discussion in the field of organic chemistry and molecular modeling.

References

[1] W. A. Smith, D. R. Lauren, E. J. Burgess, N. B. Perry, R. J. Martin, A silychristin isomer and variation of flavonolignan levels in milk thistle (*Silybum marianum*) fruits, Planta Med. 71 (2005) 877.

[2] D. Y. W. Lee, Y. Liu, Molecular structure and stereochemistry of silybin A, silybin B, isosilybin A, and isosilybin B, isolated from *Silybum marianum* (milk thistle), J. Nat. Prod. 66 (2003) 1171.

[3] N. C. Kim, T. N. Graf, C.M. Sparacino, M.C. Wani, E.W. Wall, Complete isolation and characterization of silybins and isosilybins from milk thistle (*Silybum marianum*), Org. Biomol. Chem. 1 (2003) 1684.

[4] D. Y. W. Lee, Y. Liu, in: F.Shahidi, C.T. Ho (Eds.), Phenolics in Foods and Natural Health Products, ACS Symposium Series, 909 (2005) 19.

[5] F. Kvasnicka, B. Biba, R. Sevcik, M. Voldrich, J. Kratka, Analysis of the active components of silymarin, J. Chromatogr. A 990 (2003) 239.

[6] P. Kidd, K. Head, A review of the bioavailability and clinical efficacy of milk thistle phytosome: a silybin-phosphatidylcholine complex (Siliphos®), Altern. Med. Rev. 10 (2005) 193.

[7] L. Mollison, L. Totten, J. Flexman, M. Beaman, R. Batey, Randomized double blind placebo-controlled trial of a Chinese herbal therapy (CH100) in chronic hepatitis C, J. Gastroenterol. Hepatol. 21 (2006) 1184.

[8] K. E. Mayer, R. P. Myers, S. S. Lee, Silymarin treatment of viral hepatitis: a systematic review, J. Viral Hepat. 12 (2005) 559.

[9] V. Kren, D. Walterova, Silybin and silymarin–new effects and applications, Biomed. Pap. 149 (2005) 29.

[10] J. I. Lee, B. H. Hsu, D. Wu, J. S. Barrett, Separation and characterization of silybin, isosilybin, silydianin and silychristin in milk thistle extract by liquid chromatography-electrospray tandem mass spectrometry, J. Chromatogr. A 1116 (2006) 57.

[11] Á. Kuki, L. Nagy, Gy. Deák, M. Nagy, M. Zsuga, S. Kéki, An improved high performance liquid chromatographic-mass spectrometric method for the detection of silymarin constituents, Chromatographia, 75 (2012), 175.

[12] K. Wang, H. Zhang, L. Shen, Q. Du, J. Li, Rapid separation and characterization of active flavanolignans of *Silybum marianum* by ultra-performance liquid chromatography coupled with electrospray tandem mass spectrometry, J. Pharm. Biomed. Anal. 53 (2010) 1053.

[13] N. A. Khan, H. Wu, Analysis of silymarin extracted from a commercial dosage by combining liquid-liquid extraction with negative electrospray tandem mass spectrometry, Rapid Commun. Mass Spectrom. 18 (2004) 2960.

[14] T. M. Ding, S. J. Tian, Z. X. Zhang, D. Z. Gu, Y. F. Chen, Y. H. Shi, Z. P. Sun, Validated optimized method for simultaneous analysis of active silymarin components and dimethyl-4,4′-dimethoxy-5,6,5′,6′-dimethylene dioxybiphenyl-2,2′-dicarboxylate in a pharmaceutical preparation by use of a monolithic silica C18 column, J. Pharm. Biomed. Anal. 26 (2001) 155.

[15] M. Shibano, A. S. Lin, H. Itokawa, K. H. Lee, Separation and characterization of active flavanolignans of Silybum marianum by liquid chromatography connected with hybrid ion-trap and time-of-flight mass spectrometry (LC-MS/IT-TOF), J. Nat. Prod. 70 (2007) 1424.

[16] S. Kéki, K. Tóth, M. Zsuga, R. Ferenczi, S. Antus, (+)-Silybin, a pharmacologically active constituent of *Silybum marianum*: fragmentation studies by atmospheric pressure chemical ionization quadrupole time-of-flight tandem mass spectrometry, Rapid Commun. Mass Spectrom. 21 (2007) 2255.

[17] A. Kahol, K. Singh, S. Tandon, S. Kumar, Process for isolation of hepatoprotective agent silymarin from the seeds of the plant *Silybum marianum*, (2001) Indian Patent 06309678.

[18] F. Derwa, E. D. Pauw, P. Natalis, New basis for a method for the estimation of secondary ion internal energy-distribution in soft ionization techniques, Org. Mass Spectrom.26 (1991) 117.

[19] X. H. Guo, M. C. Duursma, P. G. Kistemaker, N. M. M. Nibbering, K. Vekey, L. Drahos, R. M. Heeren, Manipulating internal energy of protonated biomolecules in electrospray ionization Furier transform ion cyclotron resonance mass spectrometry, J. Mass Spectrom. 38 (2003) 597.

[20] A. Memboeuf, A. Nasioudis, S. Indelicato, F. Pollreisz, Á. Kuki, S. Kéki, OF van den Brink, K. Vékey, L. Drahos, Size effect on fragmentation in tandem mass spectrometry, Anal. Chem. 82 (2010) 2294.

[21] Á. Kuki, L. Nagy, A. Memboeuf, L. Drahos, K. Vékey, M. Zsuga, S. Kéki, Energy-dependent collision-induced dissociation of lithiated polytetrahydrofuran: effect of the size on the fragmentation properties, J. Am. Soc. Mass Spectrom. 21 (2010) 1753.

[22] Schrodinger, LLC. Products–MacroModel. Available online: http://www.schrodinger.com/Products/macromodel.html (accessed on 13 January 2012).

[23] M. J. Frisch, G. W. Trucks, H. B. Schlegel, G. E. Scuseria, M. A. Robb, J. R. Cheeseman, G. Scalmani, V. Barone, B. Mennucci, G. A. Petersson, H. Nakatsuji, M. Caricato, X. Li, H. P. Hratchian, A. F. Izmaylov, J. Bloino, G. Zheng, J. L. Sonnenberg, M. Hada, M. Ehara, K. Toyota, R. Fukuda, J. Hasegawa, M. Ishida, T. Nakajima, Y. Honda, O. Kitao, H. Nakai, T. Vreven, J. A. Montgomery, Jr., J. E. Peralta, F. Ogliaro, M. Bearpark, J. J. Heyd, E. Brothers, K. N. Kudin, V. N. Staroverov, T. Keith, R. Kobayashi, J. Normand, K. Raghavachari, A. Rendell, J. C. Burant, S. S. Iyengar, J. Tomasi, M. Cossi, N. Rega, J. M.

Millam, M. Klene, J. E. Knox, J. B. Cross, V. Bakken, C. Adamo, J. Jaramillo, R. Gomperts, R. E. Stratmann, O. Yazyev, A. J. Austin, R. Cammi, C. Pomelli, J. W. Ochterski, R. L. Martin, K. Morokuma, V. G. Zakrzewski, G. A. Voth, P. Salvador, J. J. Dannenberg, S. Dapprich, A. D. Daniels, O. Farkas, J. B. Foresman, J. V. Ortiz, J. Cioslowski, D. J. Fox, Gaussian 09, Revision B.01, 2010, Gaussian, Inc., Wallingford CT.

[24] U. Varetto, MOLEKEL 5.4., 2009, Swiss National Supercomputing Centre: Manno, Switzerland.

Legends for Schemes and Figures

Scheme 1

Chemical structures of the main constituents in *Silybum marianum* extract.

Scheme 2

Mechanism of formation of the di-keto fragment ion *m/z* 301 from the silybins and the isosilybins.

Fig 1

Survival yield (SY) *versus* collision energy (CE) curves for the seven silymarin components. The curves are marked with squares for the silychristins (**1**, **3**) and circles for silydianin (**2**), the silybins (**4**, **5**) and the isosilybins (**6**, **7**).

Fig 2

(a) Product ion spectra (MS/MS) of the silymarin constituents recorded at the characteristic collision energies which correspond to about 50% survival yield (CE_{50}).
(b) Product ion spectra (MS/MS) of the silymarin constituents recorded at about 1% survival yield (CE_{01}): silychristin A (**1**), silydianin (**2**), silybin A (**4**) and isosilybin A (**6**).

Fig 3

Breakdown diagrams for the fragment ions *m/z* 301, *m/z* 451 and *m/z* 453 of silybin A (**4**) (filled points) and isosilybin A (**6**) (empty points). Relative intensity was calculated as the ratio of the intensity of a given product ion to that of all the product plus precursor ions.

Fig 4

3D view of the most stable conformers of silybin A (**4**) (left) and isosilybin A (**6**) (right) in an energy plot.

Fig 5

Breakdown diagrams for the product ions formed from (a) silychristin A (**1**), (b) silydianin (**2**), (c) silybin A (**4**) and (d) isosilybin A (**6**).

Table 1 The characteristic collision energy for each silymarin component. (CE_{50}: at which the intensity of the precursor ion is equal to the sum of that of all the fragment ions.) The values were measured by collision energy dependent MS/MS experiments, the standard deviation is 0.1 eV.

Peak no.	Component	CE_{50} (eV)
1	silychristin A	14.2
2	silydianin	19.4
3	silychristin B	14.2
4	silybin A	19.4
5	silybin B	19.0
6	isosilybin A	19.2
7	isosilybin B	19.4

Table 2 List of fragments mentioned in the article.

Measured (Theoretical) *m/z*	**From the analyte**	**Elemental composition**	**Proposed Structure**
125.024 (125.024)	silybins isosilybins silychristins silydianin	$C_6H_5O_3$	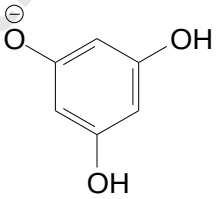
151.002 (151.004)	silybins isosilybins silychristins silydianin	$C_7H_3O_4$	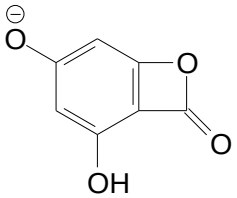
152.012 (152.012)	silybins isosilybins	$C_7H_4O_4$	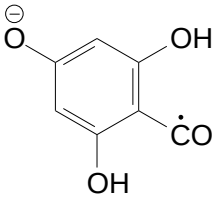
178.997 (178.999)	silybins isosilybins silychristins silydianin	$C_8H_3O_5$	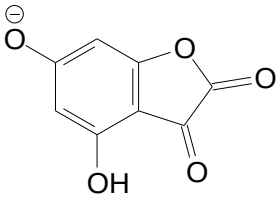
180.003 (180.006)	silybins isosilybins	$C_8H_4O_5$	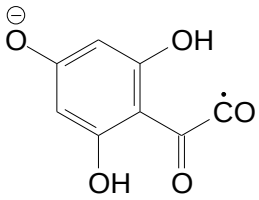

301.030 (301.035)	silybins isosilybins	$C_{15}H_9O_7$	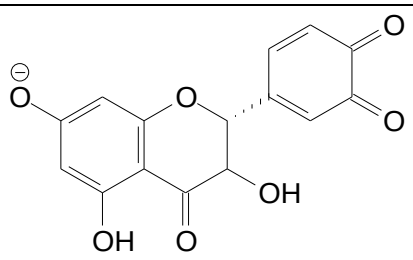
355.079 (355.082)	silychristins	$C_{19}H_{15}O_7$	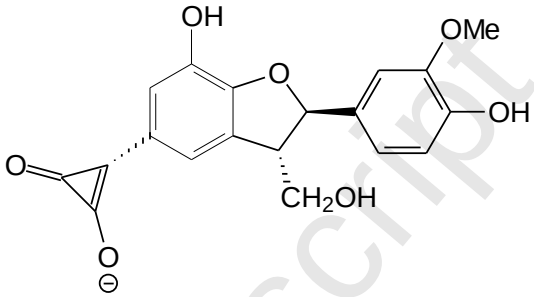
433.090 (433.093)	silychristins	$C_{24}H_{17}O_8$	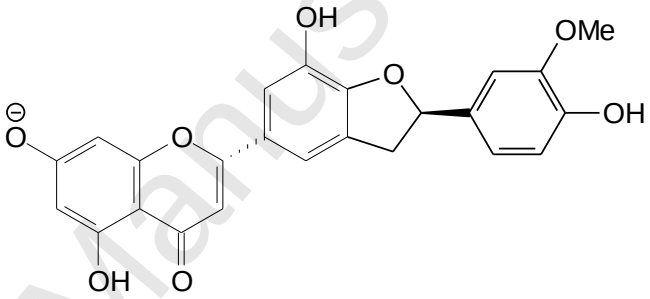
451.101 (451.103)	silybins	$C_{24}H_{19}O_9$	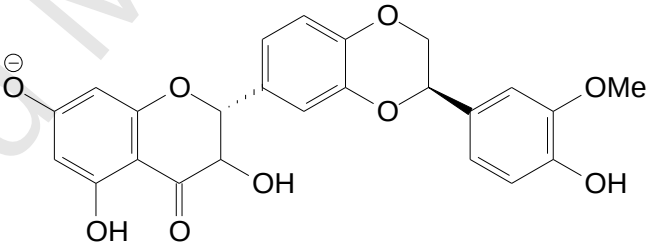
451.105 (451.103)	silychristins	$C_{24}H_{19}O_9$	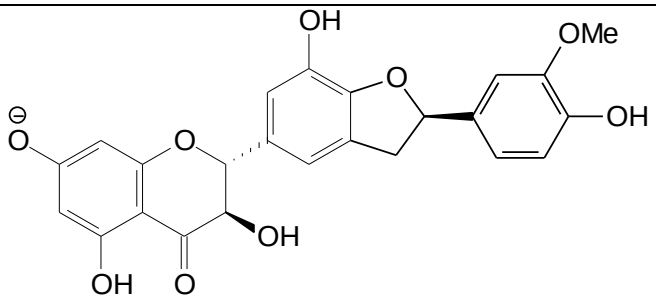
453.116 (453.119)	silybins isosilybins silychristins silydianin	$C_{24}H_{21}O_9$	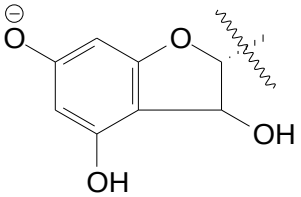
463.101 (463.103)	silybins isosilybins silychristins silydianin	$C_{25}H_{19}O_9$	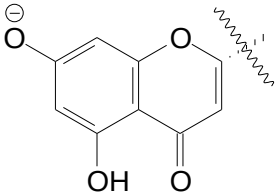

Table 3 Relative B3LYP energies of the most stable conformers of silybin A (**4**) and isosilybin A (**6**)

Ring C	Ring D	E (kJ/mol) silybin A (**4**)	E (kJ/mol) isosilybin A(**6**)
diequatorial	diequatorial	0.0	0.0
diequatorial	diaxial	16.8	13.3
diaxial	diequatorial	25.6	25.0
diaxial	diaxial	**33.1**	**60.6**

Scheme 1

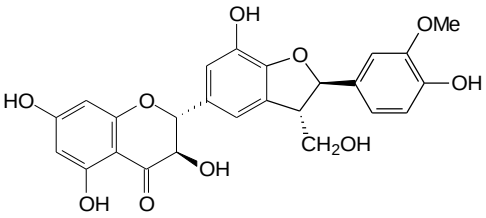

silychristin A (**1**)

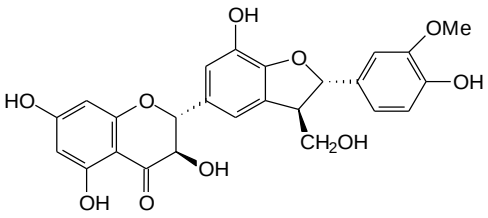

silychristin B (**3**)

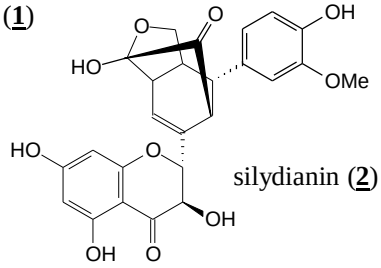

silydianin (**2**)

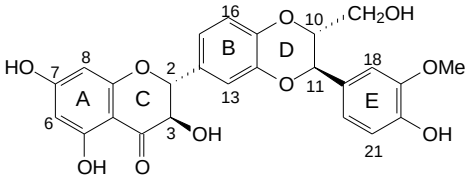

silybin A (**4**)

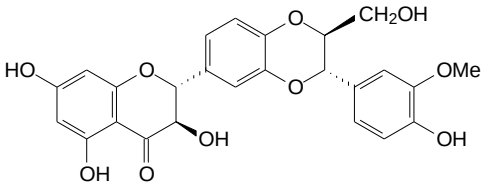

silybin B (**5**)

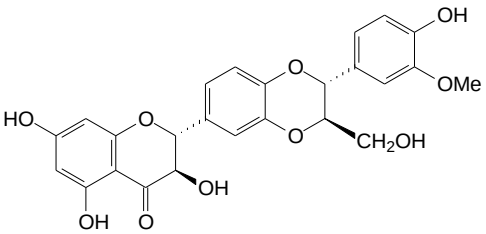

isosilybin A (**6**)

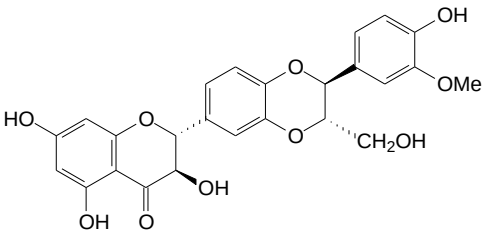

isosilybin B (**7**)

Scheme 2

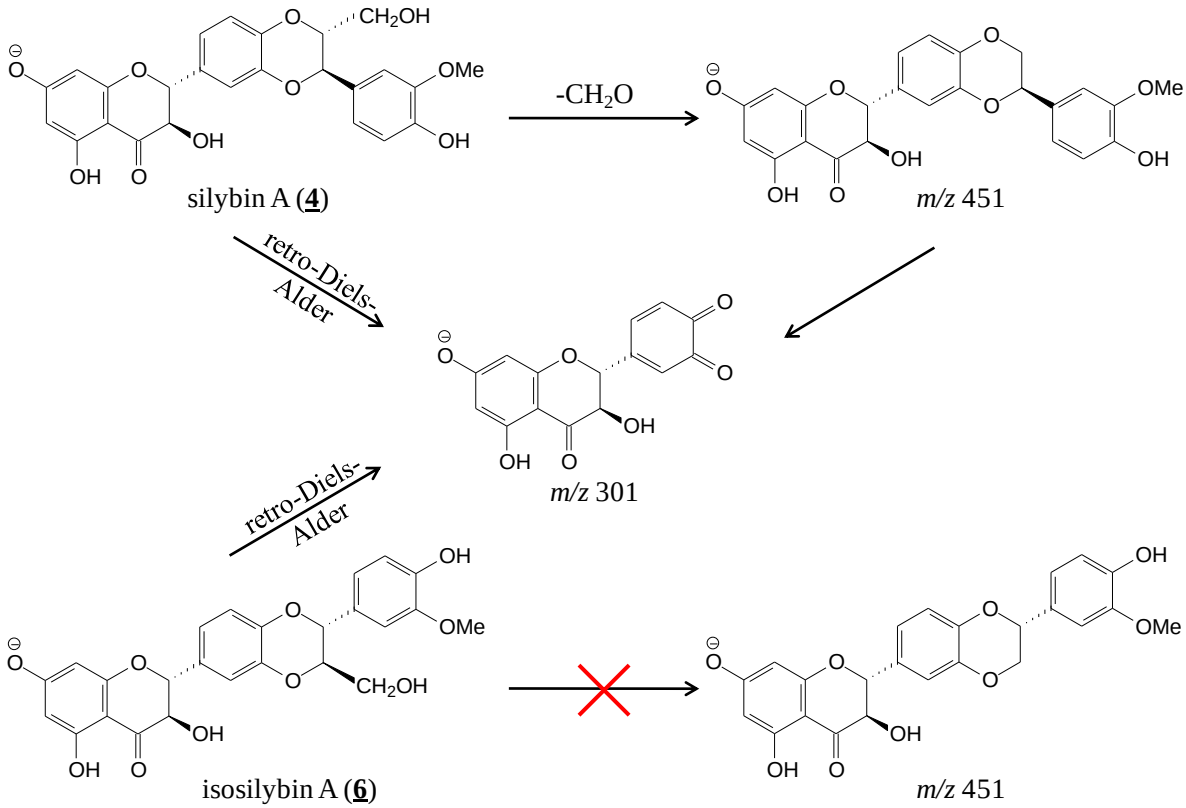

Fig 1

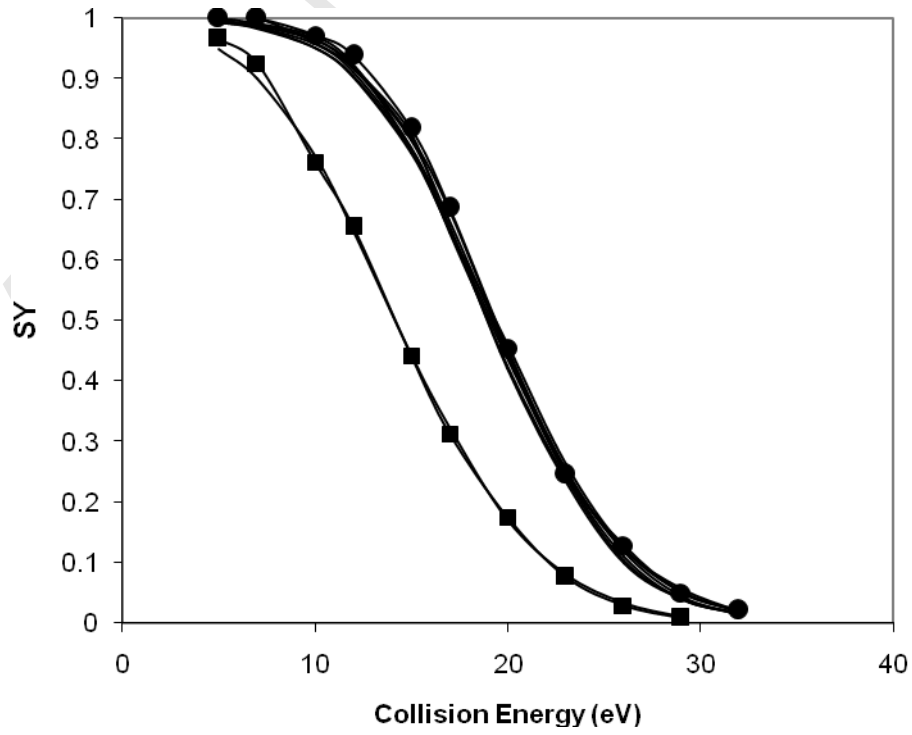

Fig 2

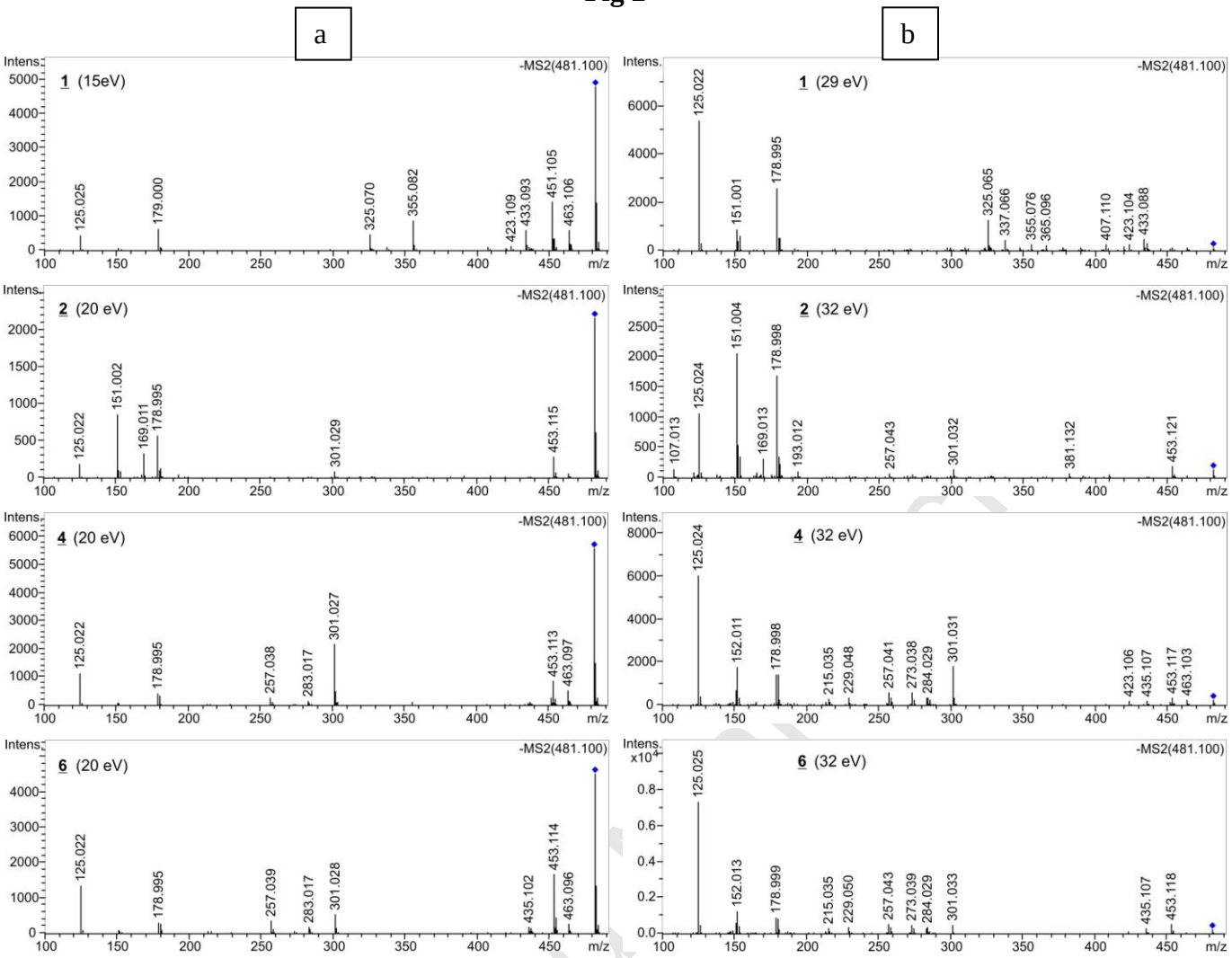

Fig 3

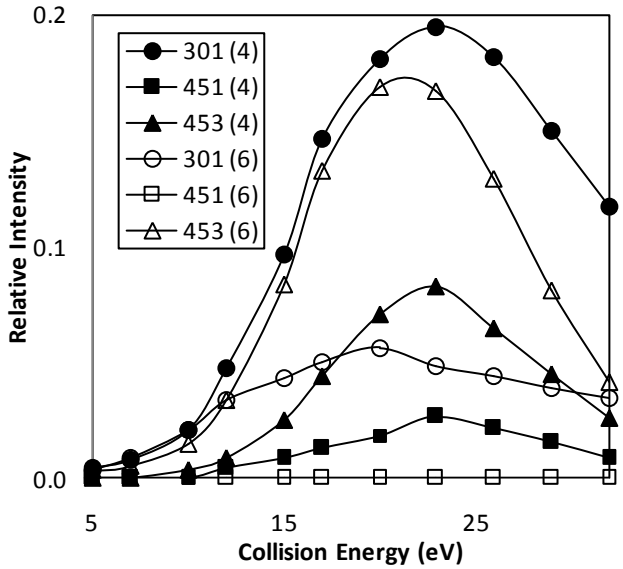

Fig 4

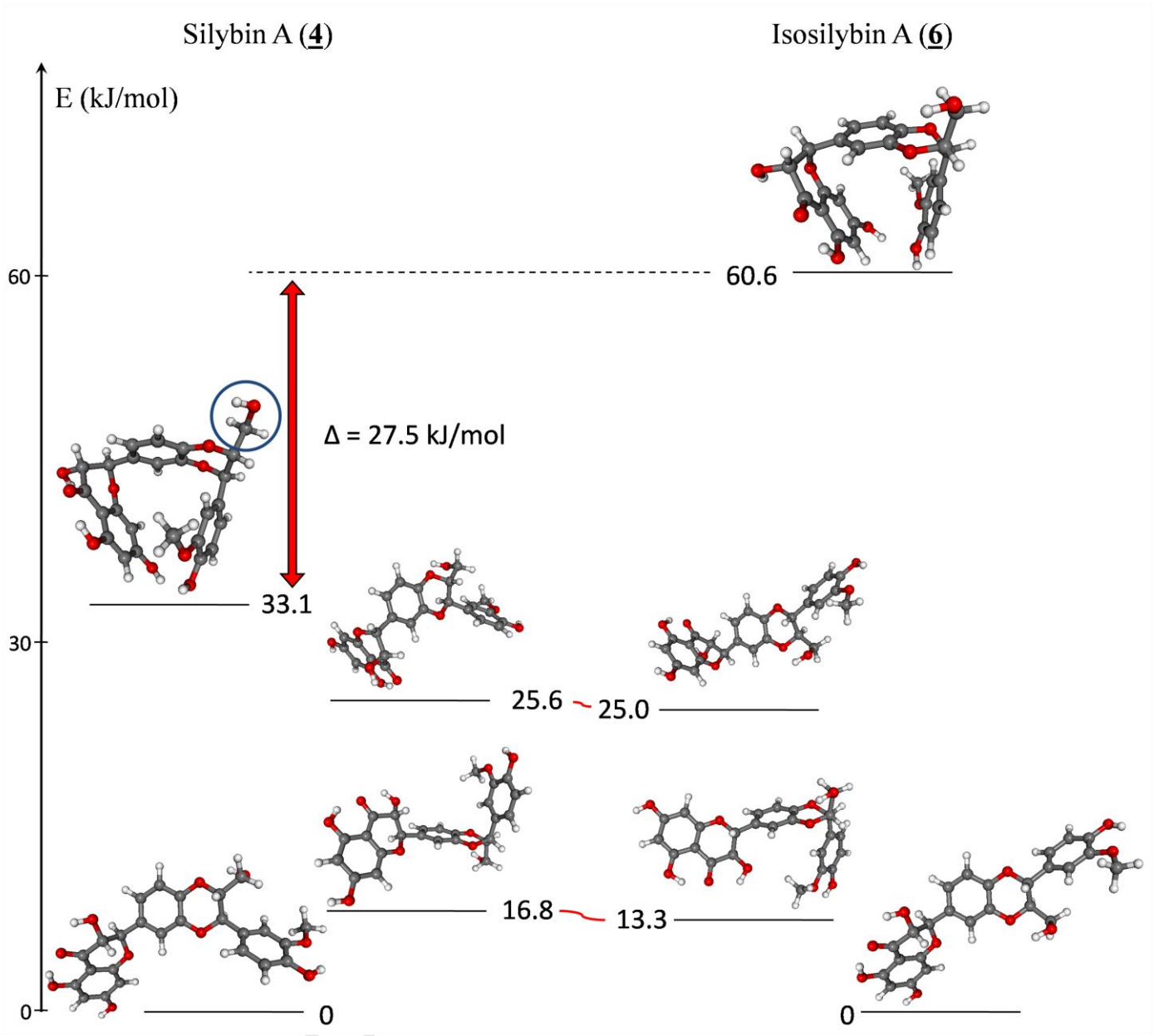

Fig 5

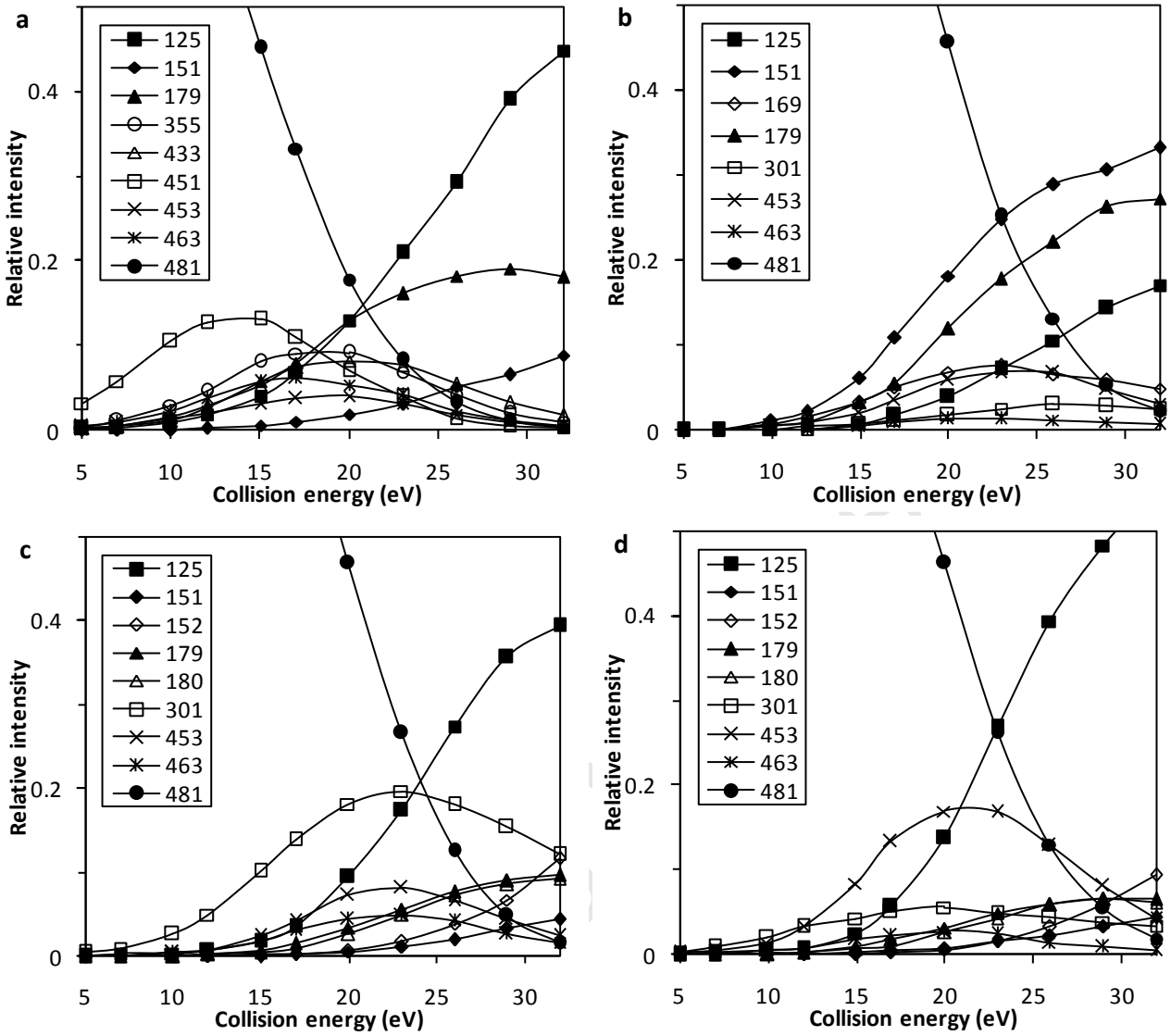

Highlights

- Energy dependence of the fragmentation of the silymarin components is reported.
- Survival yield and breakdown curve plots are presented.
- Distinct fragmentation behavior of silybins and isosilybins was observed.
- In the basis of MS/MS experiments and conformational analysis the observations were explained.